Chalmers Publication Library

Copyright Notice

©2011 IEEE. Personal use of this material is permitted. However, permission to reprint/republish this material for advertising or promotional purposes or for creating new collective works for resale or redistribution to servers or lists, or to reuse any copyrighted component of this work in other works must be obtained from the IEEE.

Chen, X., Kildal, P-S., Lai, S-H. (2011) Estimation of average Rician K-factor and average mode bandwidth in loaded reverberation chamber. *IEEE Antennas and Wireless Propagation Letters*, vol. 10, pp. 1437-1440.

http://dx.doi.org/10.1109/LAWP.2011.2179910

Estimation of Average Rician K-Factor and Average Mode Bandwidth in Loaded Reverberation Chamber

Xiaoming Chen, Per-Simon Kildal, *Fellow, IEEE*, and Sz-Hau Lai

***Abstract*—A well-stirred reverberation chamber without noticeable direct coupling between the transmitting and receiving antennas emulates an isotropic Rayleigh fading environment and can therefore be used for qualitative over-the-air (OTA) measurements of wireless devices with small nondirective antennas. By loading such a chamber, it is possible to generate a Rician environment. This letter introduces an average Rician K-factor that describes the reverberation chamber better than the normal K-factor, in particular when the chamber is provided with platform and polarization stirring. This letter shows how to estimate this average K-factor. The average mode bandwidth also changes by loading the chamber. While the average K-factor determines uncertainty, the average mode bandwidth determines the channel coherence bandwidth. They are therefore the two most important parameters for the characterizations of a reverberation chamber.**

***Index Terms*—Coherence bandwidth, K-factor, mode bandwidth, reverberation chamber.**

I. Introduction

REVEBERATION chambers are basically metal cavities with many excited modes that are stirred to create statistical environments with Rayleigh fading [1]. It has been used to measure antenna radiation efficiency and diversity gains [2], [15]. Reverberation chambers can also be used to measure total radiated power and total isotropic sensitivity of active mobile phones [3] [4]. For such measurements, the delay spread and the coherence bandwidth of the fading environment in the reverberation chamber are of importance. Delay spread and coherence bandwidth in a reverberation chamber are presented in [5] and [6]. In [5], it is also shown that the coherence bandwidth and the average mode bandwidth are almost identical when properly defined, and the relation between the coherence bandwidth and the rms delay spread was found.

The reverberation chamber can also be used to emulate Rician fading environments [7], where line-of-sight (LOS) components are present. In antenna efficiency measurements, an LOS component represents residual error that degrades measurement accuracy [8]. However, in active measurements, i.e., communication between mobile terminal and base station, Rician fading environments could be desirable in order to emulate realistic suburban or rural multipath environments. As a result, it is important to determine the K-factor in a reverberation chamber. In [7], different methods to control K-factor are studied and presented, but they are limited to fixed antennas pointing toward each other. While most of the methods are valid only for large directive antennas, loading of the chamber will also work for nondirective small antennas. In this letter, different loadings in the form of absorbing objects are located in a reverberation chamber to emulate Rician environments. However, the purpose of this letter is to introduce an average K-factor that is particularly suited for characterizing reverberation chambers provided with platform stirring [9] and polarization stirring [10], so that the orientations of the transmit and receive antennas in the chamber are not uniquely defined. We show how this average K-factor can be determined, and how it affects the average mode bandwidth and the coherence bandwidth. The approach is valid when the antennas in the chamber are small and nondirective.

The reverberation chamber used for the present measurements is the Bluetest High Performance reverberation chamber with a size of $1.8 \times 1.7 \times 1.2$ m^3. A sketch of it is shown in Fig. 1. In the Bluetest reverberation chamber, there are three

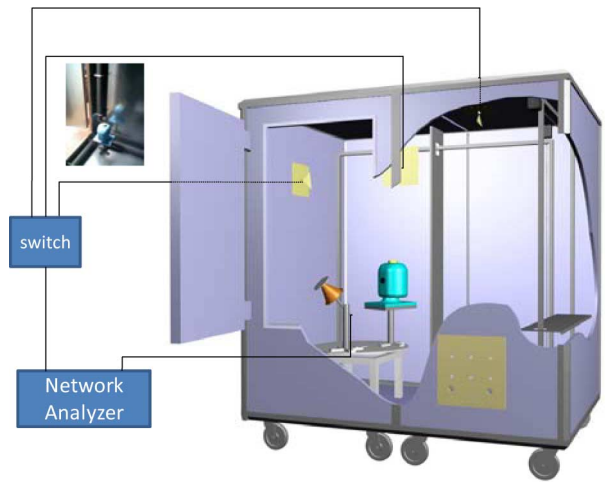

Fig. 1. Drawing of Bluetest reverberation chamber with two mechanical plate stirrers, platform and polarization stirring, shown with open door and two walls partly removed. The measurement setup with vector network analyzer and switch to the three wall antennas is shown as well, in addition to the wideband disk-cone antenna and head phantom on the platform. The inserted photograph in the top left corner shows the head phantom and the location of the three absorber-filled PVC cylinders of load2 configuration.

Manuscript received August 28, 2011; revised October 10, 2011 and November 21, 2011; accepted December 08, 2011. Date of publication December 15, 2011; date of current version December 26, 2011. This work was supported in part by the Swedish Governmental Agency for Innovation Systems (VINNOVA) within the VINN Excellence Center Chase and the Swedish Foundation for Strategic Research (SSF) within the Strategic Research Center Charmant.

X. Chen and P.-S. Kildal are with the Department of Signals and Systems, Chalmers University of Technology, Gothenburg 412 96, Sweden (e-mail: xiaoming.chen@chalmers.se; per-simon.kildal@chalmers.se).

S.-H. Lai is with the Department of Microtechnology and Nanoscience, Chalmers University of Technology, Gothenburg 412 96, Sweden.

Color versions of one or more of the figures in this letter are available online at http://ieeexplore.ieee.org.

Digital Object Identifier 10.1109/LAWP.2011.2179910

1536-1225/$26.00 © 2011 IEEE

wall antennas mounted on three orthogonal walls used for polarization stirring [10]. The antenna under test (AUT) is placed on a platform, which will rotate during measurements, referred to as platform stirring [9]. Two metallic plates are used as mechanical plate stirrers. They can move along corresponding walls either simultaneously, or sequentially, meaning one stepwise after the other in a specific sequence. In addition, certain lossy objects are used to control the fading environment. In this letter, we use five loading configurations. The empty reverberation chamber is denoted *load0*. The head phantom filled with brain-equivalent liquid is *load1*. *load2*, *load3*, and *load4* correspond to the head phantom plus three, six, and nine polyvinyl chloride (PVC) cylinders filled with microwave foam absorbers, respectively. The three lossy cylinders of each group are located along three orthogonal corners of the chamber in such a way that they cover all directions equally much, as shown in the inserted photograph at the upper left corner of Fig. 1.

II. K-Factor

Normally, in a rich scattering multipath environment, if there is no LOS or direct coupling, the channel response can be assumed to have Rayleigh fading distribution; if there is a LOS component, the channel response will have Rician fading distribution [11]. Being an essential parameter of the Rician distribution, the normal K-factor is for measurements in the reverberation chamber defined as [7], [11]

$$K = P_{\mathrm{d}}/P_{\mathrm{s}}$$
$$P_{\mathrm{d}} = |\overline{S_{21}}|^2 \quad P_{\mathrm{s}} = \overline{|S_{21} - \overline{S_{21}}|^2} \tag{1}$$

where P_{d} is the power of the LOS component $\overline{S_{21}}$ of the total transfer function S_{21}, and P_{s} is the power of the statistical scattering components of S_{21}. The total transfer function S_{21} is most conveniently measured with a vector network analyzer (VNA) between two antennas in the reverberation chamber. $\overline{S_{21}}$ means complex average of S_{21} over all stirrer positions, and $|S_{21} - \overline{S_{21}}|^2$ means the average of $|S_{21} - \overline{S_{21}}|^2$ over all stirrer positions. These averages may be evaluated over all stirring positions including platform positions and wall antennas, in which case we call it an overall or stirred-LOS K-factor. Alternatively, it may be evaluated for each platform and wall antenna position by doing the averaging only over plate positions. In this case, we get several K-factors, each one for a specific LOS component (fixed transmit and receive antennas) in the chamber, so we refer to them as stationary-LOS K-factors. These stationary-LOS K-factors will of course be different due to the different positions of orientations of the AUT. Therefore, we find it convenient in Section III to define an average stationary-LOS K-factor based on these values.

Note that in a reverberation chamber, unstirred multipath components may also appear if the stirrers are not very effective [7]. Such unstirred components are deterministic and show up in the measurement in the same way as a direct coupling or LOS component. Since both the unstirred and LOS components have the same effects on the reverberation chamber performance, we will not discuss them separately in this letter, and simply refer to both of them as apparent direct-coupled components. Thus, P_{d} in (1) is the apparent direct-coupled power.

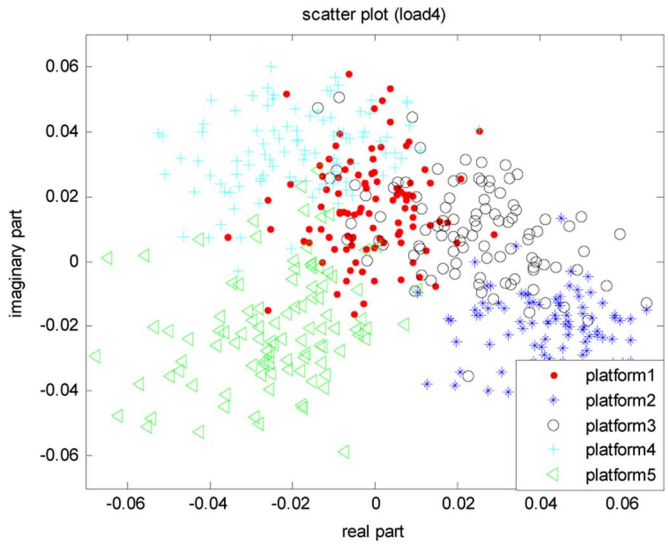

Fig. 2. Stirrer plots of S_{21} for the load4 configuration, for five platform positions and 100 plate positions per platform position, at 900 MHz.

In order to illustrate the K-factor more clearly, the platform is moved to five positions spaced by $360°/5 = 72°$, and for each platform position, each of the two stirrer plates move sequentially to 10 positions, each distributed evenly along the total distance they can move. Thereby, $10 \times 10 = 100$ plate stirrer configurations are created for each platform position. The number of platform positions was limited to five in order to reduce measurement time. At each stirrer position and for each wall antenna, a frequency sweep is performed by the VNA. Therefore, for each frequency, there are 1500 samples in total. Fig. 2 shows plots of the complex channel transfer function S_{21} between the AUT and one of the wall antennas only, at 900 MHz, for load4. The points in each group represent the channel transfer function as a function of plate stirrer position. We see that, for the loaded chamber, the channel transfer function generates five distinguishable groups, one for each platform position. This means that each platform position has a stationary-LOS K-factor (corresponding to each wall antenna) corresponding to the center of the complex S_{21} cloud at each platform position. The other loading configurations show the same tendency that the S_{21} clouds separate more and more with increasing loading, but they are not included in this letter for brevity. This means that the stationary-LOS K-factor for each of the platform positions increases with increasing loading.

III. Average Stationary-LOS K-Factor

When the reverberation chamber is provided with platform and polarization stirrings, it is convenient to define an average stationary-LOS K-factor in the following way. For each wall antenna and platform position, we calculate P_{d}, P_{s}, and the K-factor by using (1). Thereafter, we obtain the average K-factor, obtained by averaging (or simply summing) P_{d} and P_{s} over the five platform positions and three wall antennas, and using

$$K_{\mathrm{av}} = \sum P_{\mathrm{d}} / \sum P_{\mathrm{s}}. \tag{2}$$

This form of the average stationary-LOS K-factor, where we actually average P_{d} and P_{s} separately (not their ratio), is justified because P_{s} is supposed to be constant and independent of the antennas' position and orientation in the chamber according to Hill's transmission formula [12]. Therefore, we get a better estimate of true P_{s} by averaging the estimates for each platform position and wall antenna.

Such calculated average stationary-LOS K-factors are shown in Fig. 3(a). To reduce their statistical variations due to the finite number of stirrer positions, both P_{d} and P_{s} were smoothed over a sliding window of 20 MHz before being plotted. The average K-factors are slightly decreasing with increasing frequency in contrast to the K-factors in [7] that increase with frequency. The reason is that the authors of [7] used directive horn antennas as both transmitting and receiving antennas, and their gains are known to increase with frequency, whereas in this letter, small nondirective antennas are used, and the slight decrease of the K-factor with frequency is probably due to the fact that the antenna efficiency decreases with increasing frequency. Fig. 3(b) shows the stirred-LOS K-factor evaluated by using all stirrer positions (indistinguishing platform positions) directly in (1), so that we evaluate the K-factor of all the 1500 complex S_{21} samples for each frequency point and loading configuration. We see that the stirred-LOS K-factors in Fig. 3(b) are much lower than in Fig. 3(a), meaning that the stirred-LOS K-factors are significantly reduced by the platform and polarization strings. This phenomenon is as expected since the stirred-LOS K-factor is calculated by treating the platform (polarization) stirring equivalently the same as the plate stirring, and the platform (polarization) stirring randomizes LOS components at different platform (wall antenna) positions (see Fig. 2), resulting in a reduction of the complex average S_{21} overall the stirrer (including platform and wall antenna) positions and consequently a reduction of the stirred-LOS K-factor [see Fig. 3(b)]. It is shown in [8] that the K-factor (loading) determines the uncertainty of the measurements, i.e., a larger K-factor (heavier loading) implies a larger measurement uncertainty. The K-factors used in [8] are estimated constant values depending on loading via Hill's formula for the stirred components [12], corresponding to a proportionality with the average mode bandwidth [5]. The average K-factor defined in this letter enables to predict the measurement uncertainty as a function of frequency in a better way [14]. Furthermore, Fig. 3 shows the necessity of introducing the average K-factor because the stirred-LOS K-factor using (1) becomes very small and too uncertain to use for any modeling.

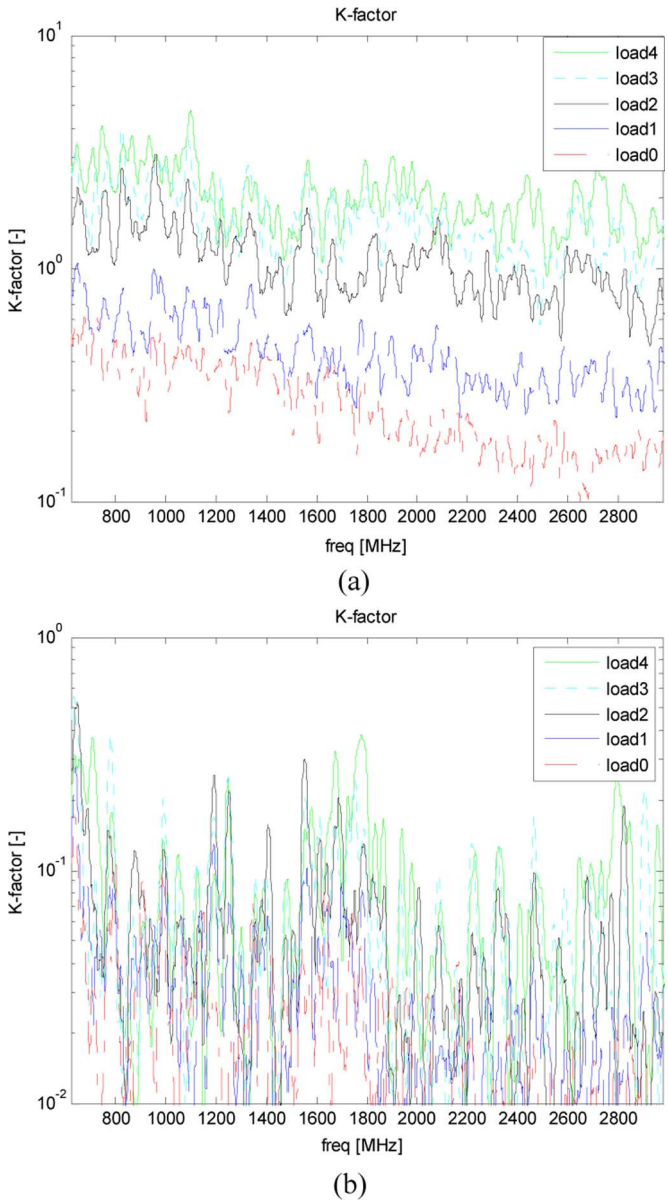

Fig. 3. (a) Average stationary-LOS K-factors according to (2). (b) Stirred-LOS K-factors calculated from all 1500 stirrer positions by using (1) directly. All curves are obtained by smoothening both P_{d} and P_{s} over 20 MHz, respectively, before evaluating the K-factors.

IV. Average Mode Bandwidth

The average mode bandwidth of the reverberation chamber, introduced in [13] based on Hill's transmission formula [12], is given as

$$\Delta f = \frac{c_0^3 e_{\mathrm{rad1}} e_{\mathrm{rad2}}}{16\pi^2 V f^2 \overline{|S_{21}|^2}} \tag{3}$$

where $\overline{|S_{21}|^2}$ is the average power transfer function of the reverberation chamber, and e_{rad1} and e_{rad2} are the total radiation efficiencies of the transmitting and receiving antennas, respectively. Equation (3) is valid when the transfer function contains enough independent samples and when there is no direct coupling. The average mode bandwidths, calculated using all the stirrer positions, are plotted in Fig. 4. Note that since the corresponding stirred-LOS K-factors (using all the stirrer positions) are small [see Fig. 3(b)], the Hill's formula (3) approximately holds.

It is shown in [5] that average mode bandwidth is the same as coherence bandwidth, but the calculation of the former is much easier than the latter. The coherence bandwidth, and its inverse, delay spread, are important parameters to characterize the channel. Therefore, the average mode bandwidth is also an important parameter for active OTA measurement (see [3]). The average mode bandwidth was presented previously in [5]. Still, it is included in this letter. The reason is that the present results are for another stirring sequence, and thereby we illustrate

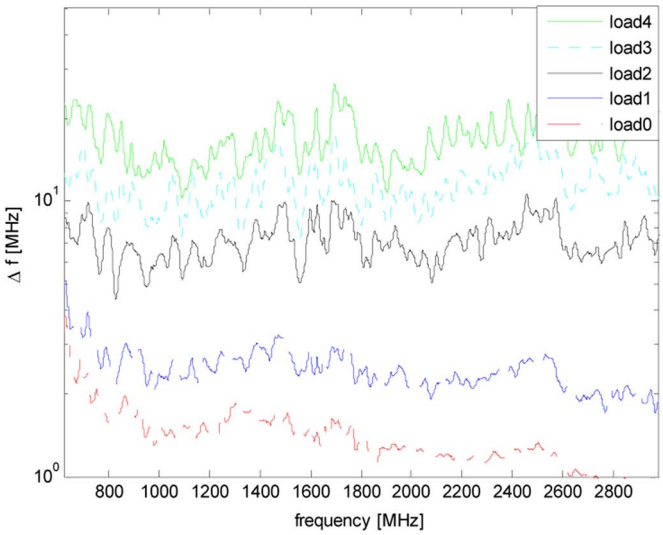

Fig. 4. Average mode bandwidths using (3) for different loading configurations. 20-MHz frequency smoothing is used.

that the average mode bandwidth is independent of string sequence as it should be (except for prediction errors). In this way, this letter also becomes more complete because the size of the average mode bandwidth is an equally important parameter as the average stationary-LOS K-factor for the characterizations of loaded reverberation chambers. Hence, we need both of these parameters. It is evident from the extensive paper [14] that they can be controlled independently.

V. Conclusion

We have defined an average stationary-LOS Rician K-factor for reverberation chambers with platform and polarization stirrings. It has been found that this average stationary-LOS K-factor can be controlled by loading the chamber, in the same way as the K-factor for a constant location and orientation of the antenna under test. However, due to platform and polarization stirrings, the overall stirred-LOS K-factor remains small for different used loadings. The average stationary-LOS K-factor and the average mode bandwidth are the most important characterizing parameters of a reverberation chamber for OTA measurements. The average mode bandwidth determines the coherence bandwidth [5] (while the latter is much more difficult to calculate) and the time delay spread, which are very important for channel characterization for active OTA measurements (see [3]). The average stationary-LOS K-factor determines the uncertainty of the measurements as shown in [8] and [14]: A larger average stationary-LOS K-factor implies a larger measurement uncertainty. However, the average K-factors used in [8] were estimated values. The calculated average stationary-LOS K-factor defined in this letter enables us to predict the measurement uncertainty as a function of frequency in a much better way [14].

References

[1] P.-S. Kildal and K. Rosengren, "Correlation and capacity of MIMO systems and mutual coupling, radiation efficiency and diversity gain of their antennas: Simulations and measurements in reverberation chamber," *IEEE Commun. Mag.*, vol. 42, no. 12, pp. 102–112, Dec. 2004.

[2] K. Rosengren and P.-S. Kildal, "Radiation efficiency, correlation, diversity gain and capacity of a six-monopole antenna array for a MIMO system: Theory, simulation and measurement in reverberation chamber," *Inst, Elect. Eng. Proc., Microw. Antennas Propag.*, vol. 152, pp. 7–16, 2005.

[3] C. Orlenius, P.-S. Kildal, and G. Poilasne, "Measurement of total isotropic sensitivity and average fading sensitivity of CDMA phones in reverberation chamber," in *Proc. IEEE AP-S Int. Symp.*, Washington, DC, Jul. 2005, vol. 1A, pp. 409–412.

[4] C. Orlenius, M. Franzen, P.-S. Kildal, and U. Carlberg, "Investigation of heavily loaded reverberation chamber for testing of wideband wireless units," in *Proc. IEEE AP-S Int. Symp.*, Albuquerque, NM, 2006, pp. 3569–3572.

[5] X. Chen, P.-S. Kildal, C. Orlenius, and J. Carlsson, "Channel sounding of loaded reverberation chamber for over-the-air testing of wireless devices—Coherence bandwidth and delay spread versus average mode bandwidth," *IEEE Antennas Wireless Propag. Lett.*, vol. 8, pp. 678–681, 2009.

[6] O. Delangre, P. D. Doncker, M. Lienard, and P. Degauque, "Delay spread and coherence bandwidth in reverberation chamber," *Electron. Lett.*, vol. 44, no. 5, Feb. 2008.

[7] C. L. Holloway, D. A. Hill, J. M. Ladbury, P. F. Wilson, G. Koepke, and J. Coder, "On the use of reverberation chamber to simulate a Rician radio environment for the testing of wireless devices," *IEEE Trans. Antennas Propag.*, vol. 54, no. 11, pp. 3167–3177, Nov. 2006.

[8] P.-S. Kildal, S.-H. Lai, and X. Chen, "Direct coupling as a residual error contribution during OTA measurements of wireless devices in reverberation chamber," in *Proc. IEEE AP-S Int. Symp.*, 2009, pp. 1–4.

[9] K. Rosengren, P.-S. Kildal, C. Carlsson, and J. Carlsson, "Characterization of antennas for mobile and wireless terminals in reverberation chambers: Improved accuracy by platform stirring," *Microw. Opt. Technol. Lett.*, vol. 30, no. 20, pp. 391–397, Sep. 2001.

[10] P.-S. Kildal and C. Carlsson, "Detection of a polarization imbalance in reverberation chambers and how to remove it by polarization stirring when measuring antenna efficiencies," *Microw. Opt. Technol. Lett.*, vol. 32, no. 2, pp. 145–149, Jul. 20, 2002.

[11] T. S. Rappaport, *Wireless Communications—Principles and Practice*, 2nd ed. Upper Saddle River, NJ: Prentice-Hall, 2002, pp. 196–202.

[12] D. A. Hill, M. T. Ma, A. R. Ondrejka, B. F. Riddle, M. L. Crawford, and R. T. Johnk, "Aperture excitation of electrically large, lossy cavities," *IEEE Trans. Electromagn. Compat.*, vol. 36, no. 3, pp. 169–178, Aug. 1994.

[13] U. Carlberg, P.-S. Kildal, and J. Carlsson, "Study of antennas in reverberation chamber using method of moments with cavity Green's function calculated by Ewald summation," *IEEE Trans. Electromagn. Compat.*, vol. 47, no. 4, pp. 805–814, Nov. 2005.

[14] P.-S. Kildal, X. Chen, C. Orlenius, M. Fransén, and C. L. Patané, "Characterization of reverberation chambers for OTA measurements of wireless devices: Formulation of channel matrix and uncertainty," *IEEE Trans. Antennas Propag.*, Oct. 2011, submitted for publication.

[15] K. Rosengren and P.-S. Kildal, "Erratum," *Inst. Elect. Eng. Proc., Microw., Antennas Propag.*, vol. 153, no. 4, p. 400, Aug. 2006.